공학석사 학위논문

Highly Reliable Quinone-Based Cathodes and Cellulose Nanofiber Separators: Toward Eco-Friendly Organic Lithium Batteries

신뢰성이 높은 퀴논 계열 양극재와 셀룰로오스 나노파이버 분리막: 친환경적인 유기 리튬 배터리를 위해서

2019 년 8 월

서울대학교 대학원

융합과학부 나노융합전공

유 가 영

Highly Reliable Quinone-Based Cathodes and Cellulose Nanofiber Separators: Toward Eco-Friendly Organic Lithium Batteries

지도 교수 김 연 상

이 논문을 공학석사 학위논문으로 제출함
2019 년 8 월

서울대학교 대학원
융합과학부 나노융합전공
유 가 영

유가영의 공학석사 학위논문을 인준함
2019 년 6 월

위 원 장 박 원 철 (인)

부위원장 김 연 상 (인)

위 원 유 지 영 (인)

Abstract

Highly Reliable Quinone-Based Cathodes and Cellulose Nanofiber Separators: Toward Eco-Friendly Organic Lithium Batteries

Gayeong Yoo
Program in Nano Science and Technology
Department of Transdisciplinary Studies
Graduate School of Convergence Science and Technology
Seoul National University

Recently, the organic compounds have been considered as promising candidates for the next generation of energy storage systems to overcome the disadvantages of the conventional inorganic cathode materials such as low specific capacities and disposal problem. Especially, Pillar[5]quinone (P5Q) is very effective for the use of the active sites that it is able to be favorable to Li uptake and implements a high theoretical capacity. Herein, I proposed that the cathodes were fabricated using the P5Q enveloped in Multi-walled Carbon Nanotubes (MWCNTs) and Cellulose Nanofibers (CNFs) with simple vacuum filtering, solving the issues of high solubility in aprotic electrolytes and low conductivity of organic compounds. Furthermore, CNFs were introduced as an alternative to the convectional polyolefin separators. The CNF separator showed less capacity fading as well

as the improvements in the ionic conductivity (0.88 mS cm^{-1}), electrolyte wettability (electrolyte uptake: 333.41 %, porosity: 70±5 %), and thermal shrinkage, in comparison to convectional polyolefin separators. Li metal battery with the suggested P5Q cathode and CNF separator exhibited highly stable capacity retention (76.5 % after 50 cycles at 0.2 C rate) and good rate capability.

Keywords : Organic lithium batteries, Cellulose Nanofibers, Carbon frame, Eco-friendly LIBs, Next generation batteries

Student Number : 2017-20994

Table of Contents

List of Figures

Figure 12. DSC (Differential Scanning Calorimetry) diagram of CNF, PP/PE/PP and PE to compare thermal stability.

Figure 13. Before and after the thermal shrinkage test of CNF ((a), (d)), PP/PE/PP ((b), (e)) and PE ((c), (f)) separator at 150 ℃ for 5 min.

Figure 14. Symmetrical cell test (Li//Li) of CNF, PP/PE/PP and PE separator with the current density of 1mA/cm^2 and 1mAh.

Figure 15. The voltage hysteresis at 1mA cm^{-2} of CNF, PP/PE/PP, PE separators.

Figure 16. Electrochemical impedance spectra of full cells with PMC cathode in the frequency range of 1 MHz to 0.1 Hz.

Figure 17. (a) Cyclic voltammogram (CV) of a PMC electrode of various voltage ranges (1.8−3.3 V, 1.7−3.3 V, 1.6−3.3 V) at a scan rate of 0.2 mV s^{-1}, (b) the initial Galvanostatic discharge curves of CNF, PP/PE/PP and PE separators with PMC cathode within the voltage range of 1.6−3.3 V.

Figure 18. Cycle performance of PMC electrode using PMC electrode as a cathode, Li metal as an anode and each CNF, PP/PE/PP and PE separator at 0.2 C.

Figure 19. Rate capability test between 1.6 and 3.3 V with various current densities (0.2 C−0.5 C−1.0 C−2.0 C−0.2 C) using PMC electrode as a cathode, Li metal as an anode and each CNF, PP/PE/PP and PE separator.

Figure 20. Zeta potential of CNF membrane.

List of Tables

Chapter 1. Introduction

1.1. Current Trend in Cathodes

Rechargeable lithium based batteries have been widely used for portable devices such as cellular phones and laptop computers.[1-3] Those electronics are in a trend of being more multi-functionalized, and the energy storage devices within such electronics are required to have a much higher energy density. The energy storage system loaded with a high energy density will also dominate the market of large scale power systems, especially with the rapid development of electric vehicles.[4-6] Therefore, high specific capacity of lithium ion batteries (LIBs) have become one of the most important factors. Although the LIBs can offer a high gravimetric capacity of 3862 mAh g^{-1} by using lithium metal as the anodic materials[7, 8], most of cathode materials which are represented as binary or ternary lithium metal (cobalt, nickel, manganese, aluminum) oxides are mainly restricted in theoretical reversible capacity comparing to the Li metal anode. Thus, the cathode is the most vital aspect in offering the high capacity. Commonly used inorganic lithium metal oxide materials as the inorganic cathodic materials have drawbacks such as their low reversible specific capacities (< 200 mAh g^{-1})[9, 10], the limited reserves of metals and their unstable trend of price. Also, the cathodic active materials have disadvantages in that a large amount of CO_2 emission arises from the manufacturing as well as the disposal process, which is not eco-friendly.[11-13]

1.2. Introduction to Organic Compounds as Active Materials

To overcome these disadvantages, the organic compounds have recently been considered as promising candidates for the next generation of energy storage systems.[14-18] They have many obvious merits compared to the inorganic materials in high theoretical capacity (>400 mAh g^{-1}), safety, sustainability, environmental friendliness and low cost. Inorganic intercalation compounds depend on changes in metal oxidation state and the charged structure of specific counter-ions that are specific to the crystal structure of the inorganic materials. This inherently restricts the versatility of inorganic compounds. On the other hand, organic compounds based on conversion reactions can be formulated and functionalized with various synthesis methods. This allows to optimize the operating voltages of batteries by modulating the oxidation and reduction potentials. It is possible to change capacity, electron transfer rates and crystal structure by modifying the chemical structure for the needs of specific energy storage devise. In addition, they are redox active toward lithium metal as well as practically any metals like magnesium, zinc and aluminum owing to their faradaic reactions.

Especially, Pillar[5]quinone (P5Q), containing five quinone units linked by methylene bridges at para positions, does not only implement a high theoretical capacity of 446 mAh g^{-1} but also is highly effective for the use of the active sites that it is able to be favorable to Li ion uptake with conversion reaction (Figure 1).[19-21] However, those kinds of organic materials with small molecular weight have two critical issues. First, they are easy to dissolve in aprotic electrolyte such as carbonate-based solvent, leading to poor cyclability and rapid capacity fading. Second is that the low

conductivity of organic molecules themselves limits their rate performance.[22, 23] To handle these problems, several approaches have been investigated to optimize the electrolyte and modify the electrode such as room-temperature ionic liquid (RTIL)[24, 25], all-solid-state electrolyte[19, 26] and polymerization of organic compounds[20, 27-30]. However, these attempts had the limitation to solve the low electronic conductivity of active materials.

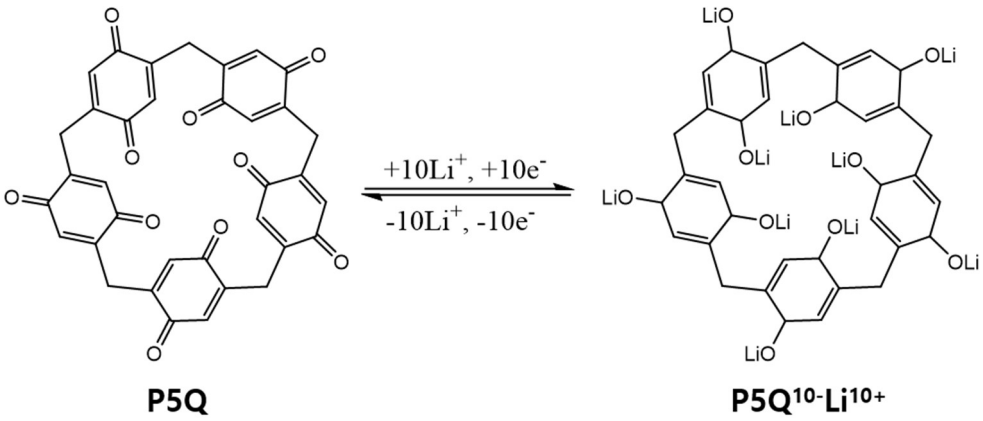

Figure 1. Structure and electrochemical redox reaction of Pillar[5]quinone (P5Q)

1.3. Pillar[5]quinone/MWCNT/CNF (PMC) Cathodes and CNF Separators

I propose a nanocomposite electrode composed of P5Q as an active material, Multi-walled Carbon Nanotubes (MWCNTs) and Cellulose Nanofibers (CNFs) to constrain the solubility of organic materials in liquid electrolyte and enhance the electronic conductivity. The MWCNTs make P5Q not dissolve in electrolyte by being entangled with P5Q and provide pathways to efficiently transport both electrons and ions because of their unique structures, which have a good electronic conductivity.[31] Also, I introduce CNFs, that are naturally abundant and sustainable mesoscopic materials as both a binder in the electrode part and a separator itself. The CNFs are well bound with P5Q in the cathode to prevent the dissolution of active materials and carry out a flexible substrate, helping to be in a film formation. It is also beneficial to use CNFs as a binder that there is no diffusion issue due to good wettability with electrolyte even though the loading level of electrode is increased. Furthermore, CNF acts as a nanoporous separator that has thermally stable structure, good ionic conductivity and wettability with electrolytes, compared with convectional polyolefin separators such as Polypropylene (PP) and Polyethylene (PE).[32-34] More importantly, the CNFs cause electrostatically repulsion with P5Q due to a slight negative charge on the surface stabilizes the surface of Li metal, suppressing the dissolution of P5Qs and contributing to the improved cycling performance better than polyolefin separators. In making the P5Q/MWCNT/CNF (PMC) cathode, I suggest vacuum filtration method instead of slurry casting method, leading to metallic current collector free and simple manufacturing process. Also, the MWCNTs performed as the current collector with the 3D structure and were in

direct contact with the active materials, which resulted in fast-charging/discharging of LIBs.

The PMC nanocomposite electrode with CNF separator (Figure 2) shows an initial capacity of 427 mAh g^{-1} at 0.2 C rate as well as highly stable capacity retention (76.5 % after 50 cycles) and good rate capability. The suggested eco-friendly organic lithium battery featuring the novelty in manufacturing of electrodes and separators for next generation can be widely used.

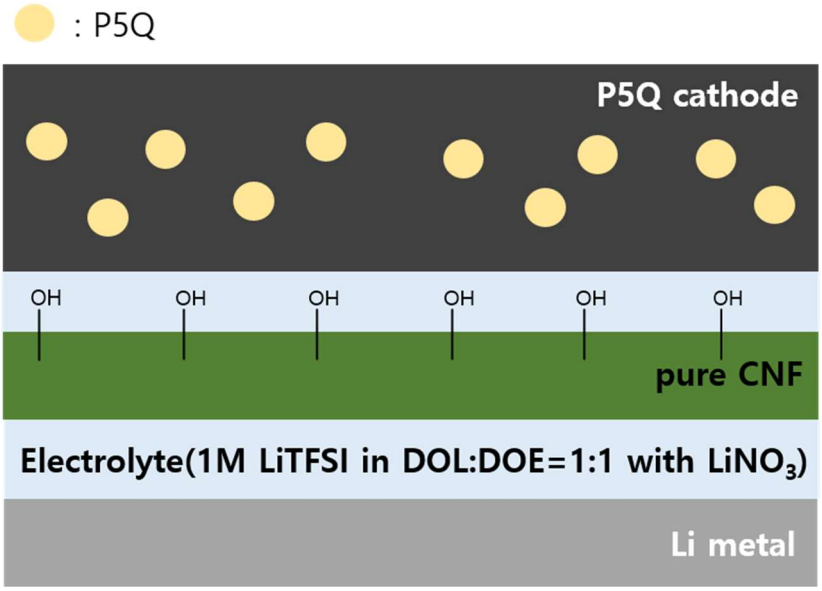

Figure 2. Schematic representation illustrating the structural features of organic-CNF batteries

Chapter 2. Experimental Section

2.1. Synthesis of 1,4-dimethoxypillar[5]arene[35]

To a solution of 1,4−dimethoxybenzene (2.764 g, 20 mmol) and paraformaldehyde (0.600 g, 20 mmol) in 1,2−dichloroethane (190 mL), trifluoroacetic acid (10 mL) was added. Reaction was refluxed for 2 h. After cooling, the reaction mixture was poured into methanol. The resulting precipitate was collected. (Figure 3(b), ~80 % Yield) ^{1}H NMR ($CDCl_3$/400 MHz): δ 6.90(s, 10H), δ 3.77(s, 10H), δ 3.75(s, 30H); ^{13}C NMR ($CDCl_3$/100 MHz): δ 150.27, δ 128.16, δ 113.17, δ 55.32, δ 29.17 (Figure 4(a))

2.2. Synthesis of Pillar[5]quinone[36]

Under Argon (Ar) atmosphere, a solution of 1,4-dimethoxypillar[5]arene (1 g, 1.3 mmol) in 100 mL of CH_2Cl_2/THF (1:1 in volume) was stirred at room temperature for 2 h. Then, ceric ammonium nitrate ($(NH_4)_2[Ce(NO_3)_6]$, 8.06 g, 14.7 mmol) in water (10 mL) was added drop by drop. The reaction mixture was stirred for 48 h to give an orange suspension. After filtration, the resulting precipitate was washed with hot water and then ethyl alcohol several times. The yellow powders were collected. (Figure 3(c), ~55 % Yield) ^{1}H NMR (trifluoroacetic acid-d/500 MHz, Figure 4(b)): δ 6.89 (s, 10H, quinone CH), δ 3.57 (s, 10H, methylene protons); ^{13}C NMR (trifluoroacetic acid-d/125 MHz, Figure 4(c)): δ 190.45 (C of carbonyl), δ 146.81 (C of quinone ring attached to methylene group), δ 138.13 (tertiary C of quinone ring), δ 28.06 (methylene C); FT-IR (Figure 4(d)): 1654 (m), 1610 (m), 1461 (s), 1377 (s), 1286 (m), 1250 (m), 1125 (m), 921 (m), 722 (m); LC-MS: m/z $[M+H]^+$ calcd for $C_{35}H_{21}O_{10}$: 601.113; found: 601.113; m/z $[M+Na]^+$ calcd for $C_{35}H_{20}O_{10}Na$: 623.095; found: 623.095

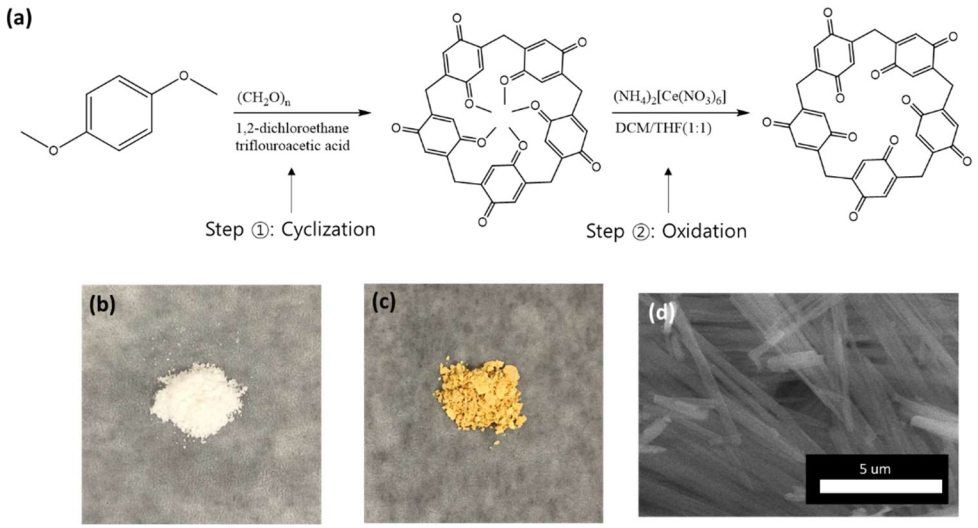

Figure 3. (a) Overall synthesis mechanism of P5Q, Pics of (b) 1,4−dimethoxypillar[5]arene and (c) Pillar[5]quinone, (d) Scanning Electron Microscopy (SEM) image of Pillar[5]quinone

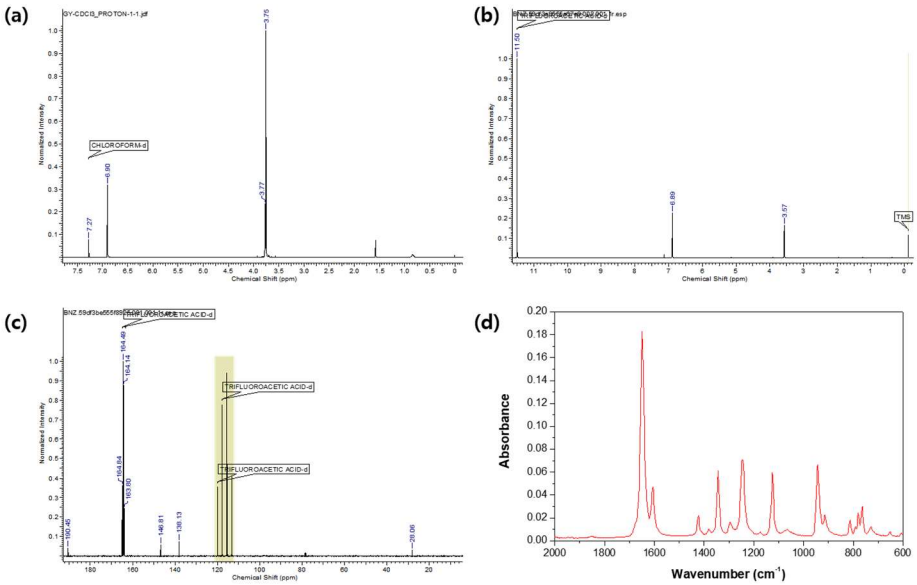

Figure 4. (a) ^{1}H− NMR of 1,4−dimethoxypillar[5]arene, (b) ^{1}H− NMR, (c) ^{13}C− NMR and (d) FT−IR of Pillar[5]quinone

2.3. Fabrication of Pillar[5]quinone/MWCNT/CNF (PMC) Nanocomposite Electrodes and Cellulose Nanofiber (CNF) Separators

The Pillar[5]quinone/MWCNT/CNF (PMC) nanocomposite electrodes were fabricated via vacuum filtration method. The P5Q, MWCNTs (CM-95, Hanwha Chemical Co., Ltd.) and aqueous gel CNFs (2.46 wt%, ANPOLY) were added in water with Sodium Dodecylbenzene Sulfonate (SDBS, Sigma-Aldrich) surfactant and tip-sonicated for 30 min. The composite dispersion was filtered using a cellulose acetate (CA) membrane (0.2 μm pore, Advantec), resulting in the formation of the PMC films. The contents of each material in PMC electrode were estimated from the Thermogravimetric Analysis (TGA). The Cellulose Nanofibers were dispersed in IPA[37] using the tip sonicator (VC-750, Sonics & Materials, Inc.) for 20 min. The solution was poured onto CA filter paper and then subjected to vacuum filtration. The CNFs films were easily peeled from the filter paper.

2.4. Material Characterizations

Pillar[5]quinone synthesized was identified with ^{1}H, ^{13}C-NMR (500 MHz, Avance-500, Bruker), Fourier-transform Infrared (FT-IR) Spectroscopy and Liquid Chromatography Mass (LC-MS) Spectrometry (6530 Q-TOF, Agilent Technologies). The CNF separators were characterized by Scanning Electron Microscopy (SEM), Differential Scanning Calorimetry (DSC), contact angles and Zeta potential (ELSZ-2000, Otsuka Electronics Co., Ltd).

2.5. Electrochemical Characterizations

The electrochemical properties were evaluated using CR2032-type coin cells that were assembled in an argon-filled glove box. The AC impedance (VSP, BioLogic Science Instruments) was performed from 0.1 HZ to 1 MHz at room temperature with an amplitude of 5 mVrms. Galvanostatic charging/discharging was tested at 0.2 C rate using battery cycler (WBCS 3000L, WonATech) and the full cells were analysed in the potential range of 1.6-3.3 V vs Li/Li^+. The symmetrical cell tests (Li/Li) were examined with a current density of 1mA cm^{-2} and 1 mAh. The electrolyte was 1M LiTFSI in the ether (DOE/DME, 1:1 in volume)-based solvent with 0.3 M $LiNO_3$ additive. The control P5Q cathode was composed of P5Q, Super P (Timcal) and PVdF (Kynar) with a weight ratio of 6:3:1 on Al foil (13 mm thick, KJCC). The olefin separators were used PP/PE/PP (Celgard 2325) and PE (NH616, Asahi Kasei) to compare with CNF separators.

Chapter 3. Results and Discussion

3.1. Fabrication and Characterization of PMC Electrodes

The synthesis to obtain P5Q was conducted in two steps and Figure 3(a) is an overall synthesis procedure of P5Q. NMR, FT-IR and LC-MS were used to confirm each material (detailed in 2.2 Synthesis of Pillar[5]quinone and Figure 4). P5Q was obtained as yellow powder and identified as a column shape particle by SEM image (Figure 3(c), Figure 3(d)).

The cathodes using P5Q as an active material were fabricated with the simple vacuum filtration method (Figure 5(a)) and attained as a freestanding membrane (Figure 5(b)), especially enabling to bend the electrode by adding CNFs (Figure 5(c)). The method has the following advantages: (1) It benefits from increasing the energy density by an elimination of the metallic current collector[38], making the electrode light and lowering the manufacturing cost, (2) It is able to increase the loading level of cathode, comparing that the slurry casting method has the limit due to cracking, (3) The networks with three dimensional (3D) structure functioned as a framework that is closely connected to the MWCNTs induce fast electron transport and efficient ion diffusion, contributing to redox kinetics[31]; and (4) Flexible LIBs can be developed with CNFs binder. The MWCNTs and CNFs in an electrode were well entangled with P5Qs and it was analysed through SEM images (Figure 6). Thermogravimetric Analysis (TGA) was used to estimate the contents of each material in PMC electrode (Figure 7). Each ratio of P5Q and MWCNT in PMC electrode was 1:1 and CNF content was at about 7 %. Although the initial capacity of cathode manufactured by slurry casting method

offered ~156 mAh g^{-1}, the PMC electrode made by vacuum filtration method showed a high initial capacity of ~382 mAh g^{-1} in the potential range of 1.8–3.3 V vs Li/Li^+ (Figure 8(a)).[19] The P5Q in cathode made by slurry casting method is easy to dissolve in electrolyte so it causes not only the low capacity from the initial capacity but also the rapid capacity fading, comparing to the capacity between 1st and 5th cycle (Figure 8(b)). However, PMC electrode is well combined with MWCNTs and CNFs, which trap the active materials and contribute to constrain the solubility of active materials in electrolyte. This outstanding result is attributed to 3D framework with a confinement effect of the well-interconnected electronic networks based on MWCNTs and CNFs, fastening the redox kinetics.[31]

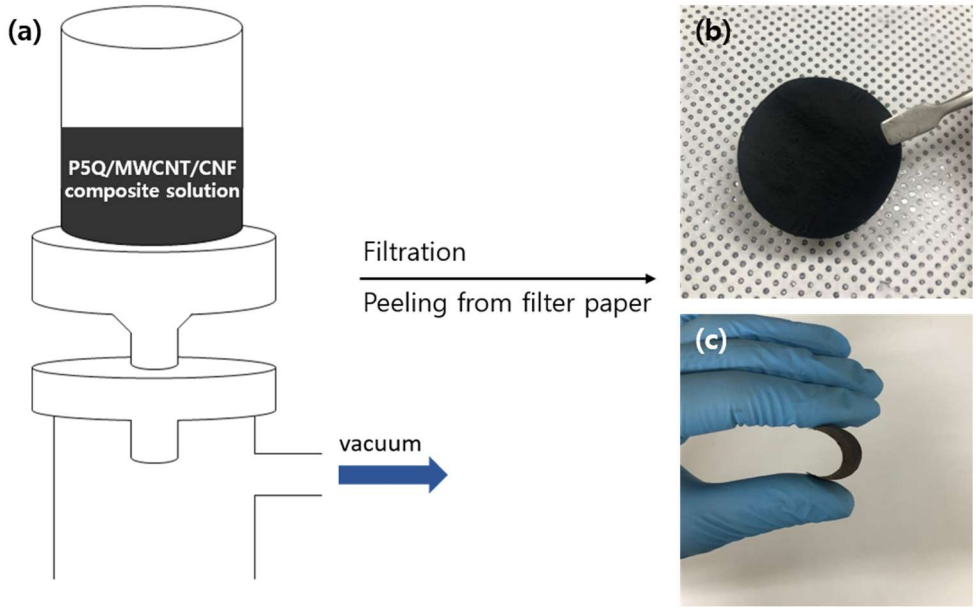

Figure 5. (a) Schematic illustration of simple vacuum filtration method, (b) and (c) photograph of PMC electrode.

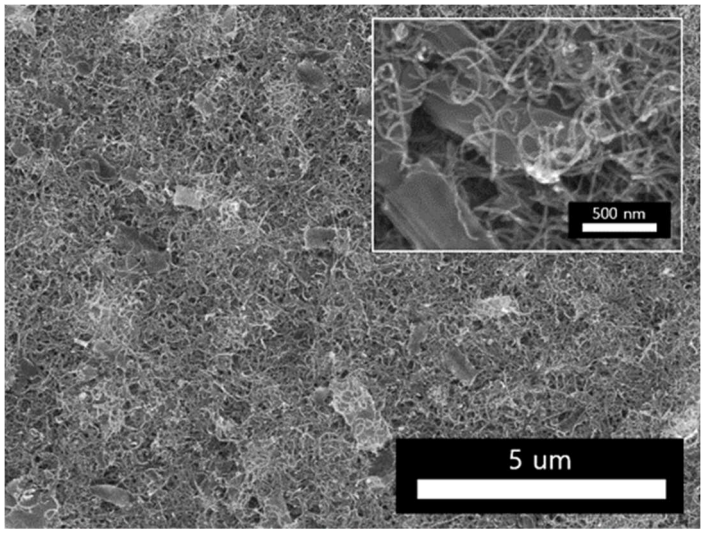

Figure 6. SEM images of the P5Q/MWCNT/CNF (PMC) composite electrode.

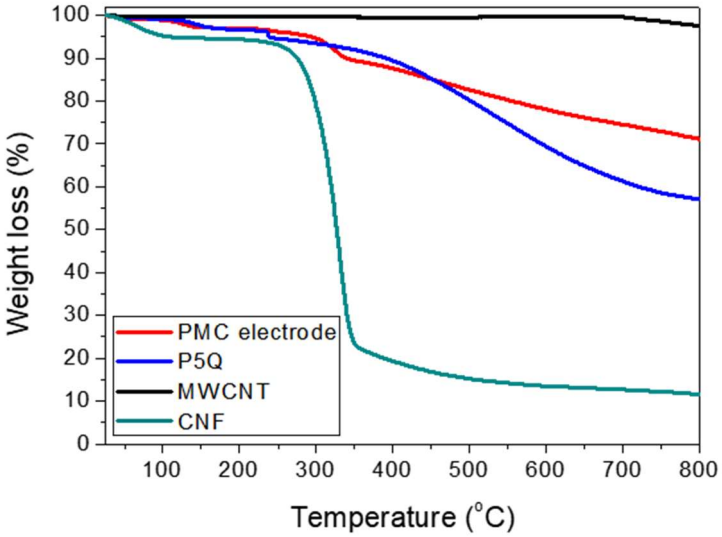

Figure 7. TGA (Thermogravimetric analysis) curve of P5Q, MWCNT, CNF and PMC cathode.

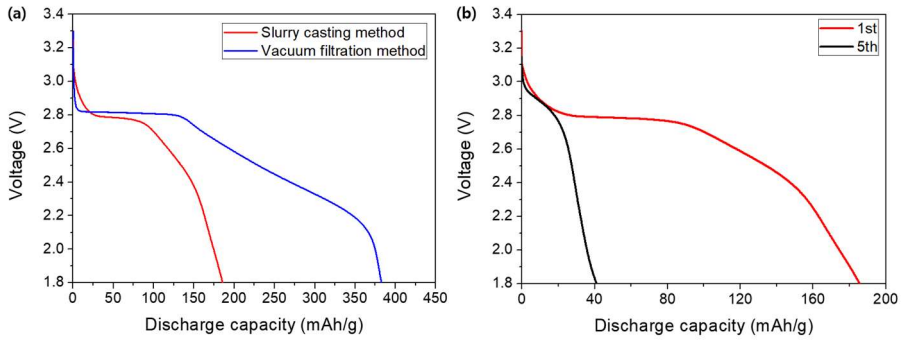

Figure 8. (a) The initial discharge curves of the cathode by slurry casting method (red line) and vacuum filtration method (blue line) with a PE separator in ether (DOE/DME, 1:1)–based solvent adding 1 M LiTFSI and 0.3 M $LiNO_3$ additive at 0.2 C rate, (b) The initial and 5th discharge curves of the cathode by slurry casting method.

3.2. Fabrication and Characterization of CNF Separators

CNFs were uniformly dispersed in a high content of IPA (97 % of IPA and 3 % of water) because the porous structure is varied by the ratio of the solvents.[37] IPA takes the fibers apart and helps to make a nanoporous channel that promotes ion transport, whereas water enhances the packing density of CNFs. The morphology of CNF separator, which was vacuum filtered, shows the highly porous structure and the pore diameter is less than 80 nm (Figure 9). This high pore tortuosity of CNF separator is expected to avoid the dendritic growth on Li metal that leads to a thermal runaway issue.[34]

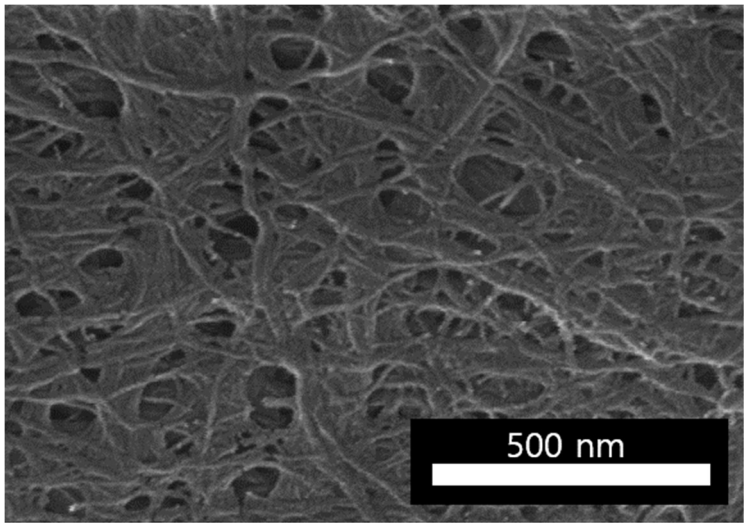

Figure 9. SEM image of Cellulose Nanofibers (CNFs) separator

3.2.1 Characterization of CNF Separator: Contact Angle, Electrolyte Uptake, Porosity and Ionic Conductivity

In order to characterize the wettability of polyolefin (PP/PE/PP and PE) and CNF separators, the contact angles of each separator are measured with the same electrolyte (1 M LiTFSI in the ether (DOE/DME)−based solvent with 0.3 M $LiNO_3$ additive). As seen on Figure 10(c), the contact angle of CNF separator cannot be calculated because CNF separator was immersed as soon as the electrolyte was dropped, while PP/PE/PP and PE separators have the contact angles of 54° and 51° respectively due to their hydrophobic property (Figure 10(a), (b)). The electrolyte uptakes of PP/PE/PP, PE and CNF separators were 138.94 wt%, 257.35 wt% and 333.41 wt% respectively, showing that the CNF separator has the most excellent electrolyte−philicity (Table. 1). In addition, this excellent wettability of CNF separator with the electrolyte can also be ascribed to much higher porosity (70±5 %) than the electrolyte with a PP/PE/PP separator (39 %[41]) or with a PE separator (46±6 %[42]). Its unique nanoporous network contributes to capillary intrusion and fast electrolyte absorption.[45] As displayed in Figure 11(a) and (b), the ionic conductivity of CNF separator (0.88 mS cm^{-1}) is better than that of the polyolefin separators (PP/PE/PP: 0.76, PE: 0.68 mS cm^{-1}).[44] It means that the CNF separator is expected to implement a better cycle performance and rate capability, providing the conducting channels for Li ions and moving a large amount of ions comfortably between cathode and anode through electrolyte.

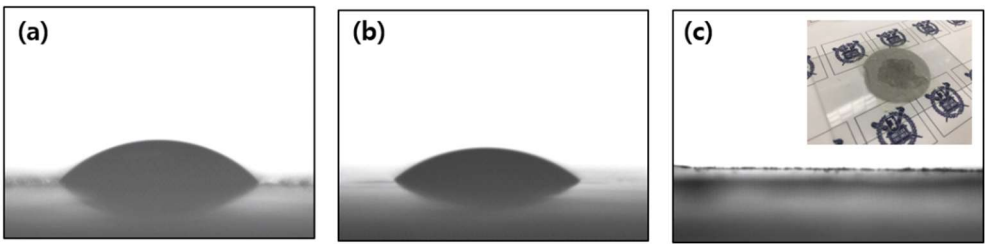

Figure 10. Contact angle of (a) PP/PE/PP, (b) PE and (c) CNF (inset. pic of CNF right after the test).

$$\text{Electrolyte uptake}\ (\%) = \frac{W_1 - W_0}{W_0} \times 100$$

W_0: The weight of dried separator

W_1: The weight of separator after soaking in the electrolyte

$$\text{Porosity}\ (\%) = \frac{W_b - W_a}{\rho_e \times V_s} \times 100$$

W_a: The weight of dried separator

W_b: The weight of separator after soaking in the electrolyte

ρ_e: The density of electrolyte (n-butanol: 0.81g/mL)

V_s: The volume of separator

Table 1. Comparison of electrolyte uptake and porosity with CNF, PP/PE/PP and PE separators.

	CNF	PP/PE/PP	PE
Electrolyte uptake (%)	333.41	138.94	257.35
Porosity (%)	70±5	39	46±6

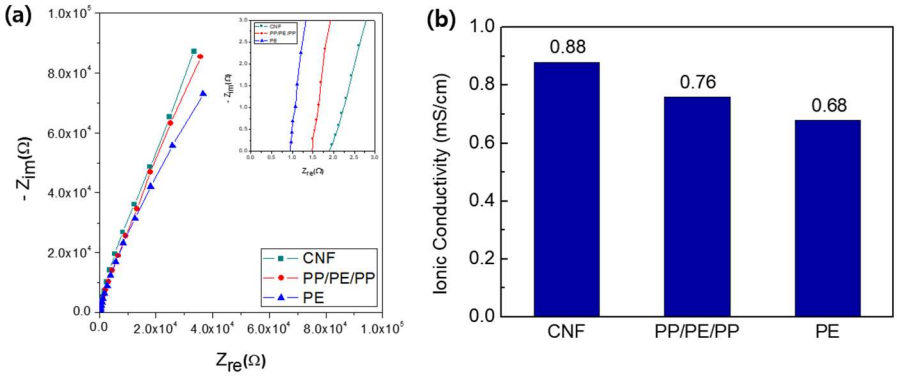

Figure 11. (a) Nyquist plot of the half cells, (b) ionic conductivity of CNF, PP/PE/PP and PE separators.

3.2.2 Thermal Stability Tests

To compare thermal characteristics of each separator, DSC analysis was conducted to examine the melting point of CNF and polyolefin separators, as shown in Figure 12. Polyolefin separators showed endothermic peaks around 135 ℃ and 163 ℃ but CNF separator did not show any peak up to 250 ℃. Thus, it is able to ensure the safety of batteries when CNFs are introduced as a separator. Thermal shrinkage test was also conducted to evaluate the thermal stability, which places each separator in a convection oven at 150 ℃ at 5 min (Figure 13). It clearly showed that CNF separator did not show any deformation and maintained their original dimension after being heated, while both PP/PE/PP and PE separators were destroyed. This indicates that CNF separators ensure the safety with regard to increasing the temperature of batteries up to 150 ℃.

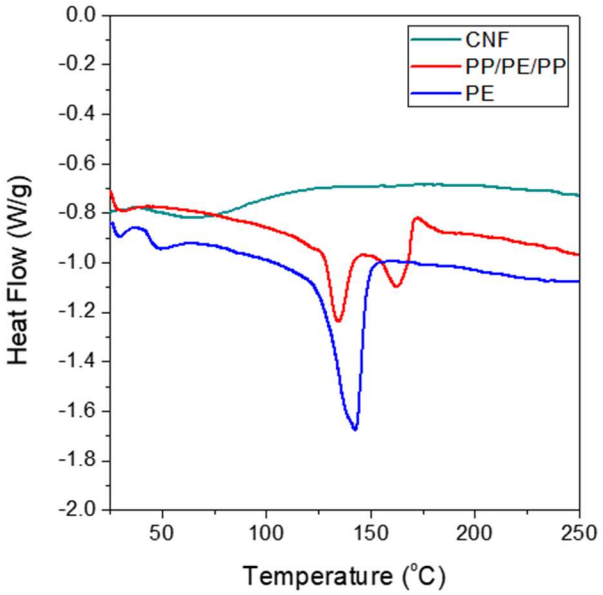

Figure 12. DSC (Differential Scanning Calorimetry) diagram of CNF, PP/PE/PP and PE to compare thermal stability.

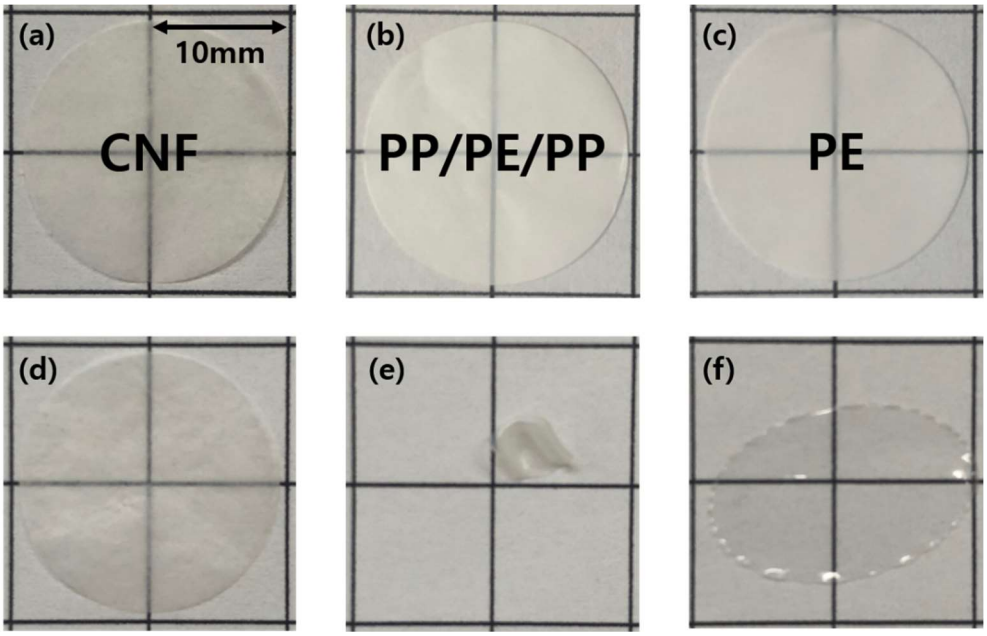

Figure 13. Before and after the thermal shrinkage test of CNF ((a), (d)), PP/PE/PP ((b), (e)) and PE ((c), (f)) separators at 150 ℃ for 5 min.

3.2.3 Symmetrical Cell tests

Symmetrical cell (Li//Li) test was carried out so as to examine the stability on the surface of Li metal with the current density of 1mA/cm^2 and 1mAh, repeating stripping and plating (Figure 14).[39, 40, 47] Polyolefin separators showed unstable profile during plating/stripping process and became overvoltage due to the increased formation of solid electrolyte interphase (SEI) layer. On the contrary, when the CNF separator was used on Li//Li symmetric cell configuration, it showed very stable behaviour even after 600 hours. The CNF separators featuring a homogeneous distribution of nano-sized pores induce a homogeneous Li^+ ion flux[48] and the unique pore tortuosity of CNFs prevents the Li dendritic growth that puncture the separator. The nanostructure constructed by CNFs can keep the structure stable in the volume expansion of the Li metal better than polyolefin separators and improve the reversibility of Li plating/stripping.

Voltage hysteresis, which is average of the difference in voltage between plating and striping of each cycle, was calculated by the following equation (Figure 15).

$$\textbf{Voltage hysteresis} = \frac{V\ max_{stripping} - V\ min_{plating}}{2}$$

With PP/PE/PP and PE separators, the inactive layer, which can be performed as the resistance, was accumulated on the surface of Li metal during the cycles and result in the ohmic potential drop at 1 mA cm^{-2}.[40] However, when CNF separator is used as a separator, a stable profile can be confirmed within the voltage range of 2 mV and 5 mV.

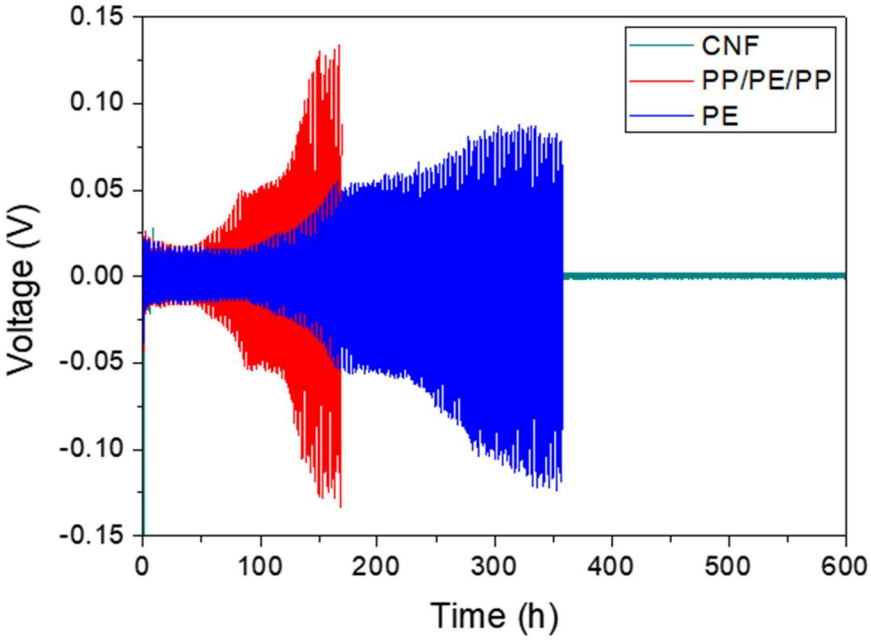

Figure 14. Symmetrical cell test (Li//Li) of CNF, PP/PE/PP and PE separators with the current density of 1mA/cm^2 and 1mAh.

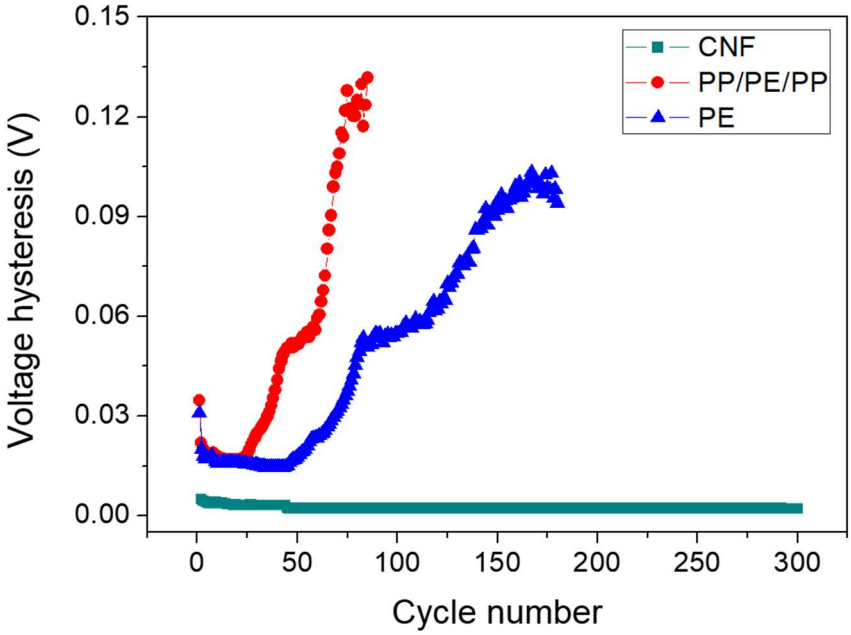

Figure 15. The voltage hysteresis at 1mA cm^{-2} of CNF, PP/PE/PP, PE separators.

3.3. Electrochemical Performances of Organic-CNF Batteries

Figure 16, 18 ,19 show the electrochemical performance of organic-lithium metal batteries with PMC electrode and CNF separator. From AC impedance (Figure 16) of full cells in the frequency range of 1 MHz to 0.1 Hz, the CNF separator has a smaller charge transfer resistance (R_{ct}) of 49.2 Ω than PP/PE/PP (59.1 Ω) and PE (59.0 Ω) separator cells.

Figure 17(a) exhibits the cyclic voltammograms (CV) of a PMC electrode of various voltage ranges (1.8-3.3 V, 1.7-3.3 V, 1.6-3.3 V) at a scan rate of 0.2 mV s^{-1}. The shape of redox peaks became sharp by widening the operating voltage range and PMC electrode ran stably even within 1.6-3.3 V. To investigate the electrochemical characteristics with each separator, a cycle performance test was conducted between 1.6 and 3.3 V at 0.2 C rate, as showed in Figure 18. The cell with CNF separator showed the high initial capacity of ~427 mAh g^{-1}, corresponding to 95.7 % of its theoretical capacity (446 mAh g^{-1}), even though PP/PE/PP and PE separators indicated ~390 mAh g^{-1} and ~387 mAh g^{-1}, respectively (Figure 17(b)). The PMC electrode displayed the plateau region from 2.9 V to 2.5 V during the discharge step. This is related to the unique structure of multi-carbonyl macrocyclic compound, with the multistep reduction of the carbonyl groups in the quinone units (Figure 1[19]). After aging for stabilization on Li metal during 5 cycles, PE/PP/PP and PP separators demonstrated specific capacity retentions of 71.6 % and 62.6 % during 50 cycles, respectively (Figure 18). On the other hand, the cell with CNF separator showed a higher specific capacity than the cell of polyolefin separators and the improved cycle stability, retaining 76.5 % of the initial capacity. In Figure 19, the rates of 0.2, 0.5, 1.0, 2.0 and 0.2 C were applied to observe the rate capability.

The battery with CNF separator rendered a good capacity retention as well as the higher capacity. This improved electrochemical performance is due to the nanostructure constructed by cellulose nanofibers, this factor offered Li^+ flexible channels.[34] Also, the surface on CNF has a slightly negative charge (~−10 mV, Figure 20)[43], so it is expected to enable the electrostatically repulsion with $P5Q^{10-}$ during the discharge process, preventing active materials from migrating to an anode part.

In spite of the fact that Pure P5Q is an electrical insulator and has the microrod shape which limits its utilization and Li^+ ion diffusion, MWCNTs enhanced the electronic conductivity and trapped the P5Q, leading to a high specific capacity and improved a cycle/rate performance.[34, 37]

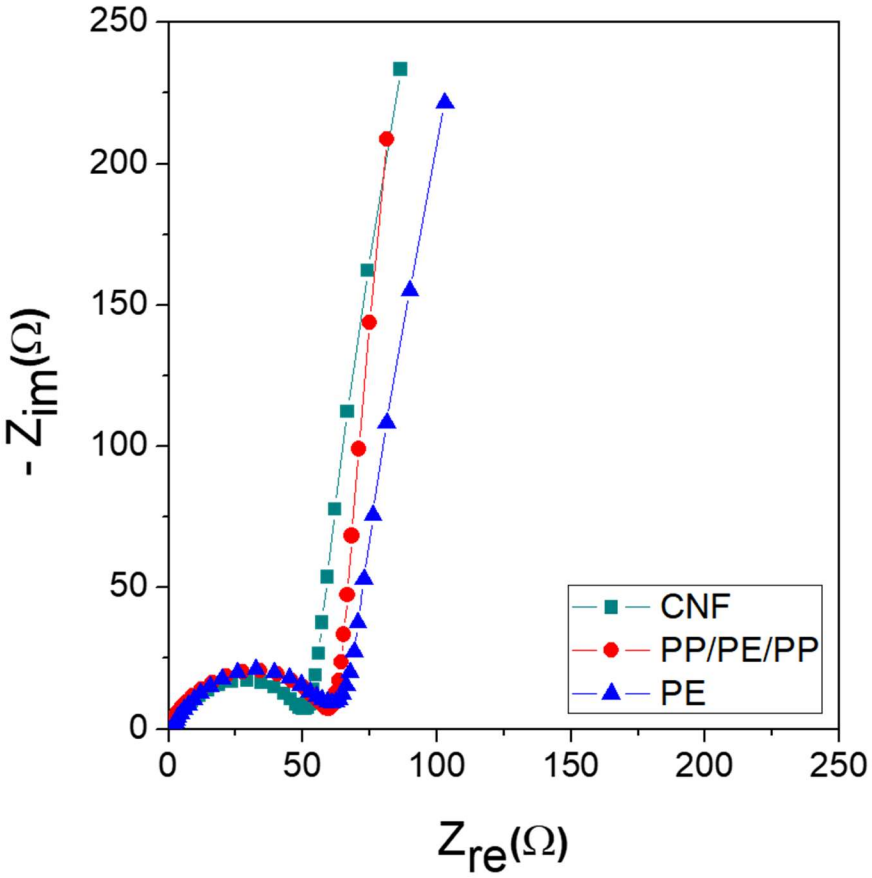

Figure 16. Electrochemical impedance spectra of full cells with PMC cathode in the frequency range of 1 MHz to 0.1 Hz.

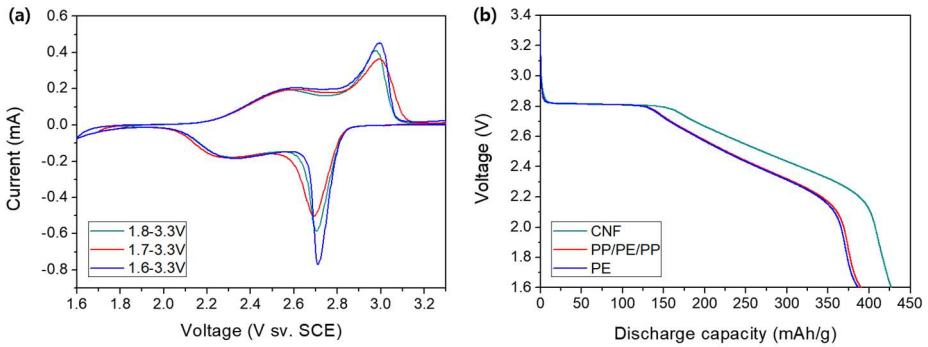

Figure 17. (a) Cyclic voltammogram (CV) of a PMC electrode of various voltage ranges (1.8–3.3 V, 1.7–3.3 V, 1.6–3.3 V) at a scan rate of 0.2 mV s^{-1}, (b) the initial Galvanostatic discharge curves of CNF, PP/PE/PP and PE separators with PMC cathode within the voltage range of 1.6–3.3 V.

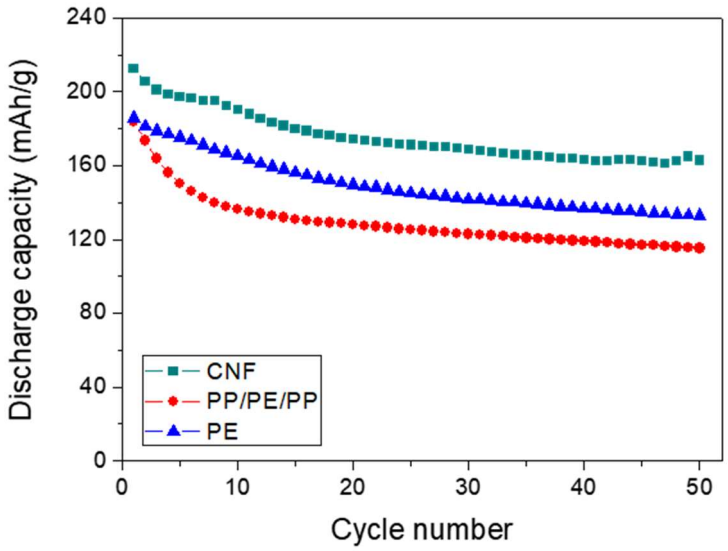

Figure 18. Cycle performance of PMC electrode using PMC electrode as a cathode, Li metal as an anode and each CNF, PP/PE/PP and PE separator at 0.2 C.

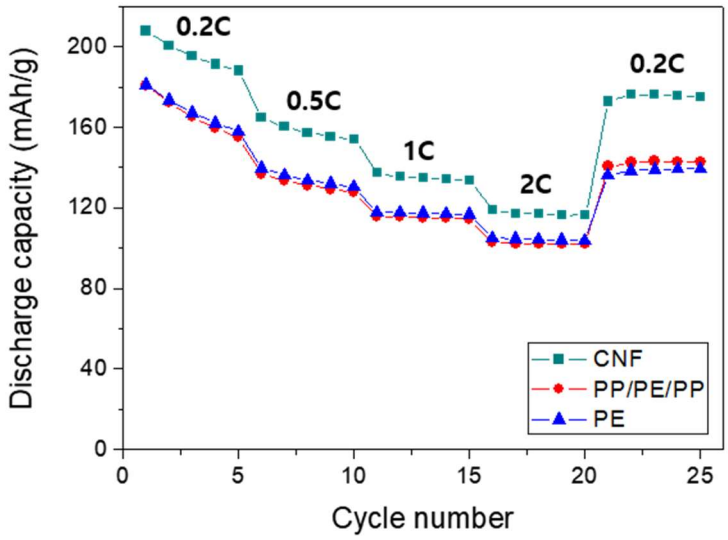

Figure 19. Rate capability test between 1.6 and 3.3 V with various current densities (0.2 C−0.5 C−1.0 C−2.0 C−0.2 C) using PMC electrode as a cathode, Li metal as an anode and each CNF, PP/PE/PP and PE separator.

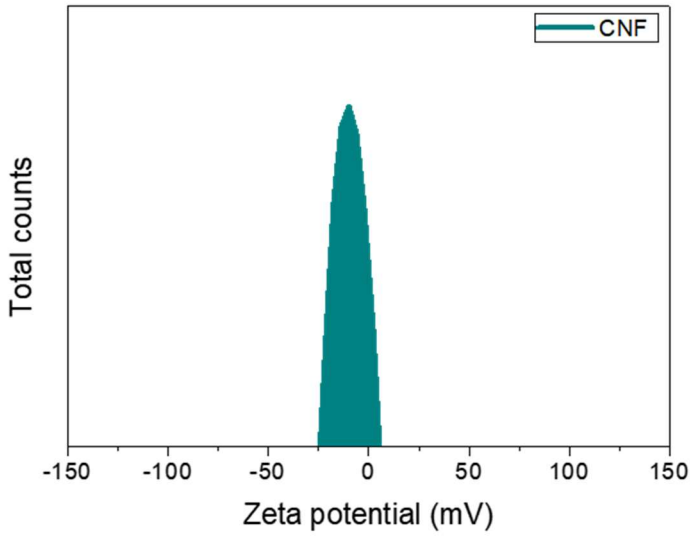

Figure 20. Zeta potential of CNF membrane.

The specific energy density (E) and power density (P) were calculated from Galvanostatic charge−discharge curves by using the following formula. The mass used in the calculation was active materials in the electrodes.

$$\text{Energy density (E)} = \frac{I}{m}\int_{t_1}^{t_2} V dt$$

$$\text{Power density (P)} = \frac{E}{t}$$

I: The discharge current (A)

V: The discharge voltage (V)

t: The discharge time (h)

m: the total mass of active materials in the electrodes (kg)

Table 2. The initial energy density and power density of CNF, PP/PE/PP and PE separators.

	CNF	PP/PE/PP	PE
Energy density (Wh/kg)	1083.52	850.71	984.47
Power density (W/kg)	130.54	110.96	111.66

Chapter 4. Conclusion

In conclusion, I have developed eco-friendly organic lithium batteries with Pillar[5]quinone as an active material and CNF separators. Organic materials are promising candidates for the next generation of energy storage systems because of high theoretical capacity, safety, sustainability, environmental friendliness and low cost. Additionally, CNF is a fabulous material for not only a binder to make flexible electrodes but also as a separator to ensure the safety issue in batteries, showing good ionic conductivity (0.88 mS cm^{-1}), electrolyte wettability (333.41 %), porosity (70±5 %) and thermal stability. The Pillar[5]quinone/MWCNT/CNF (PMC) electrode made by vacuum filtration method effectively constrained the issues of high solubility in aprotic electrolytes and low conductivity of organic cathodic compounds, compared with the convectional slurry casting method. MWCNTs lower the solubility of organic materials into electrolyte, providing pathways of both electrons and ions transportation. The cell composed of PMC cathode and CNF separator showed an initial capacity as high as 427 mAh g^{-1} with 76.5 % capacity retention after 50 cycles at 0.2 C rate. The proposed strategy can widely apply to other organic lithium metal batteries for next generation advanced batteries.

References

1. M. Armand, J.-M. Tarascon, Building better batteries. *Nature* 2008, 451, 652-657.

2. L. Li, Z. Wu, S. Yuan and X.-B. Zhang, Advances and challenges for flexible energy storage and conversion devices and systems. *Energy Environ. Sci.* 2014, 7, 2101-2122.

3. K. Kang, Y. S. Meng, J. Bréger, C. P. Grey, G. Ceder, Electrodes with High Power and High Capacity for Rechargeable Lithium Batteries. *Science* 2006, 311, 5763, 977-980.

4. J. H. Lee, C. S. Yoon, J.-Y. Hwang, S.-J. Kim, F. Maglia, P. Lamp, S.-T. Myung, Y.-K. Sun, High-energy-density lithium-ion battery using a carbon-nanotube-Si composite anode and a compositionally graded $Li[Ni_{0.85}Co_{0.05}Mn_{0.10}]O_2$ cathode. *Energy Environ. Sci.* 2016, 9, 2152-2158.

5. B. Dunn, H. Kamath, J.-M. Tarascon, Electrical Energy Storage for the Grid: A Battery of Choices. *Science* 2011, 334, 6058, 928-935.

6. J. Yan, Z. Fan, W. Sun, G. Ning, T. Wei, Q. Zhang, R. Zhang, L. Zhi, F. Wei, Advanced Asymmetric Supercapacitors Based on $Ni(OH)_2$/Graphene and Porous Graphene Electrodes with High Energy Density. *Adv. Funct. Mater.* 2012, 22, 2632-2641.

7. R. Khurana, J. L. Schaefer, L. A. Archer, G. W. Coates, Suppression of Lithium Dendrite Growth Using Cross-Linked Polyethylene/Poly(ethylene oxide) Electrolytes: A New Approach for Practical Lithium-Metal Polymer Batteries. *Chem. Soc.* 2014, 136, 7395-7402.

8. X. Wang, Y. Hou, Y. Zhu, Y. Wu, R. Holze, An Aqueous Rechargeable Lithium Battery Using Coated Li Metal as Anode. *Scientific Reports* 2013, 3, 1401.

9. B. L. Ellis, K. T. Lee, L. F. Nazar, Positive Electrode Materials for Li-Ion and Li-Batteries. *Chem. Mater.* 2010, 22, 691-714.

10. B. Scrosati, J. Garche, Lithium batteries: Status, prospects and future. J. Power Sources 2010, 195, 2419-2430.

11. K. Ishiara, 5th Ecobalance Conference, November 7, 2002, Tsukuba.

12. D. Larcher, J-M. Tarascon, Towards greener and more sustainable batteries for electrical energy storage. *Nature Chemistry* **2015**, 7, 19-29.

13. H. P. Wu, K. Wang, Y.N. Meng, K. Lu, Z.X. Wei, An organic cathode material based on a polyimide/CNT nanocomposite for lithium ion batteries. *J. Mater. Chem. A* **2013**, 1, 6366-6372.

14. H. Chen, M. Armand, G. Demailly, F. Dolhem, P. Poizot, J.-M. Tarascon, From Biomass to a Renewable $Li_XC_6O_6$ Organic Electrode for Sustainable Li-Ion Batteries. *ChemSusChem* **2008**, 1, 348-355.

15. Y. Wu, R. Zeng, J. Nan, D. Shu, Y. Qiu, S.-L. Chou, Quinone Electrode Materials for Rechargeable Lithium/Sodium Ion Batteries. *Adv. Energy Mater.* **2017**, 1700278.

16. Y. Liang, Z. Tao, J. Chen, Organic Electrode Materials for Rechargeable Lithium Batteries. *Adv. Energy Mater.* **2012**, 2, 742-769.

17. Z. Song, H. Zhou, Towards sustainable and versatile energy storage devices: an overview of organic electrode materials. *Energy Environ. Sci.* **2013**, 6, 2280-2301.

18. T. B. Schon, B. T. McAllister, P.-F. Li, D. S. Seferos, The rise of organic electrode materials for energy storage. *Chem. Soc. Rev.* **2016**, 45, 6345-6404.

19. Z. Zhu, M. Hong, D. Guo, J. Shi, Z. Tao, J. Chen, All-Solid-State Lithium Organic Battery with Composite Polymer Electrolyte and Pillar[5]quinone Cathode. *J. Am. Chem. Soc.* **2014**, 136, 16461-16464.

20. A. Ahmad, Q. Meng, S. Melhi, L.Mao, M. Zhang, B.-H. Han, K. Lu, Z. Wei, A Hierarchically Porous Hypercrosslinked and Novel Quinone based Stable Organic Polymer Electrode for Lithium-Ion Batteries. *Electrochimica Acta* **2017**, 255, 145-152.

21. L. Huan, J. Xie, Z. Huang, M. Chen, G. Diao, T. Zuo, Computational electrochemistry of Pillar[5]quinone cathode material for lithium-ion batteries. *Computational Materials Science* **2017**, 137, 233-242.

22. S. Lee, J. E. Kwon, J. Hong, S. Y. Park, K. Kang, The role of substituents in determining the redox potential of organic electrode materials in Li and Na rechargeable batteries:

electronic effects vs. substituent–Li/Na ionic interaction. *J. Mater. Chem. A* **2019**, 7, 11438.

23. W. Walker, S. Grugeon, O. Mentre, S. Laruelle, J.–M. Tarascon, F. Wudl, Ethoxycarbonyl–Based Organic Electrode for Li–Batteries. *J. Am. Chem. Soc.* **2010**, 132, 18, 6517–6523.

24. Y. Hanyu, T. Sugimoto, Y. Ganbe, A. Masuda, I. Honma, Multielectron Redox Compounds for Organic Cathode Quasi–Solid State Lithium Battery. *J. Electrochem. Soc.* **2014**, 161 (1), A6–A9.

25. Y. Hanyu, I. Honma, Rechargeable quasi–solid state lithium battery with organic crystalline cathode. *Scientific Reports* **2012**, 2, 453.

26. W. Huang, Z. Zhu, L. Wang, S. Wang, H. Li, Z. Tao, J. Shi, L. Guan, J. Chen, Quasi-Solid-State Rechargeable Lithium-Ion Batteries with a Calix[4]quinone Cathode and Gel Polymer Electrolyte. *Angew. Chem. Int. Ed.* **2013**, 52, 9162–9166.

27. M. Yao, H. Senoh, T. Sakai, T. Kiyobayashi, Redox active poly(N–vinylcarbazole) for use in rechargeable lithium batteries. *J. Power Sources* **2012**, 202, 364–368.

28. K. Liu, J. Zheng, G. Zhong, Y. Yang, Poly(2,5–dihydroxy–1,4–benzoquinonyl sulfide) (PDBS) as a cathode material for lithium ion batteries. J. Mater. Chem **2011**, 21, 4125–4131.

29. L. Zhan, Z. Song, J. Zhang, J. Tang, H. Zhan, Y. Zhou, C. Zhan, PEDOT: Cathode active material with high specific capacity in novel electrolyte system. *Electrochimica. Acta* **2008**, 53, 8319–8323.

30. Z. Song, H. Zhan, Y. Zhou, Anthraquinone based polymer as high performance cathode material for rechargeable lithium batteries. *Chem. Comm.* **2009**, 45, 448–450.

31. Z. Yin, S. Cho, D.–J. You Y.–K. Ahn, J. Yoo, Y. S. Kim, Copper nanowire/multi–walled carbon nanotube composites as all–nanowire flexible electrode for fast–charging/discharging lithium–ion battery. *Nano Research* **2018**., 11, 769–779.

32. X. Du, Z. Zhang, W. Liu, Y. Deng, Nanocellulose–based conductive materials and their emerging applications in energy devices – A review. *Nano Energy* **2017**, 35, 299–320.

33. W. Chen, H. Yu, S.–Y. Lee, T. Wei, J. Li, Z. Fan, Nanocellulose:

a promising nanomaterial for advanced electrochemical energy storage. *Chem. Soc. Rev.* 2018, 47, 2837-2972.

34. H. Zhang, X. Wang, Y. Liang, Preparation and characterization of a Lithium-ion battery separator from cellulose nanofibers. *Heliyon* 2015, 1, 2, e00032.

35. T. Boinski, A. Szumna, A facile, moisture-insensitive method for synthesis of pillar[5]arenes—the solvent templation by halogen bonds, *Tetrahedron* 2012, 68, 46, 9419-9422.

36. D. N. Shurpik, P. L. Padnya, L. I. Makhmutova, L. S. Yakimova, I. I. Stoikov, Selective stepwise oxidation of 1,4-decamethoxypillar[5]arene. *New J. Chem.* 2015, 39, 9215-9220.

37. S.-J. Chun, E.-S. Choi, E.-H. Lee, J. H. Kim, S.-Y. Lee, S.-Y. Lee, Eco-friendly cellulose nanofiber paper-derived separator membranes featuring tunable nanoporous network channels for lithium-ion batteries. *J. Mater. Chem.* 2012, 22, 16618-16626.

38. J.-H. Kim, Y.-H. Lee, S.-J. Cho, J.-G. Gwon, H.-J. Cho, M. Jang, S.-Y. Lee, S.-Y. Lee, Nanomat Li-S batteries based on all-fibrous cathode/separator assemblies and reinforced Li metal anodes: towards ultrahigh energy density and flexibility. *Energy Environ. Sci.* 2019, 12, 177-186.

39. H. Lee, J. Song, Y.-J. Kim, J.-K. Park, H.-T. Kim, Structural modulation of lithium metal-electrolyte interface with three-dimensional metallic interlayer for high-performance lithium metal batteries. *Scientific Reports* 2016, 6, 30830.

40. H. Kim, Y. J. Gong, J. Yoo, Y. S. Kim, Highly stable lithium metal battery with an applied three-dimensional mesh structure interlayer. *J. Mater. Chem. A* 2018, 6, 15540-15545.

41. Celgard® High Performance Battery Separators, http://www.celgard.com

42. NH616, Asahi Kasei Corporation, https://www.asahi-kasei.co.jp/asahi

43. P. Huang, Y. Zhao, S. Kuga, M. Wu, Y. Huang, A versatile method for producing functionalized cellulose nanofibers and their application. *Nanoscale* 2016, 8, 3753-3759.

44. Y.-k. Ahn, J. Park, D. Shin, S. Cho, S. Y. Park, H. Kim, Y. Piao,

J. Yoo, Y. S. Kim, Enhanced electrochemical capabilities of lithium ion batteries by structurally ideal AAO separator. *J. Mater. Chem. A* **2015**, 3, 10715–10719.

45. P. Arora, Z. (J.) Zhang, Battery Separators. *Chem. Rev.* **2004**, 104, 10, 4419–4462.

46. R. Pan, R. Sun, Z. Wang, J. Lindh, K. Edström, M. Strømme, L. Nyholm, Sandwich–structured nano/micro fiber–based separators for lithium metal batteries. *Nano Energy* **2019**, 55, 316–326.

국 문 초 록

신뢰성이 높은 퀴논 계열 양극재와 셀룰로오스 나노파이버 분리막 : 친환경적인 유기 리튬 배터리를 위해서

유 가 영
융합과학부 나노융합전공
서울대학교 대학원

전기차와 더불어 휴대용 전자기기에 다양한 기능을 수행하기 위해서는 높은 용량의 리튬 배터리가 필수적입니다. 높은 용량을 구현하는데 있어서 양극이 중요한 역할을 합니다. 하지만, 주로 사용하는 양극재인 무기 금속 산화물은 공급되는 가격변동 추이도 불안정하고 재사용 비율이 적으며 생산 및 처리하는 과정에서 많은 양의 이산화탄소를 배출하는 문제점이 있습니다. 그래서 이것의 대체재로 유기물에 대한 연구가 이루어지고 있는데, 이는 400mAh g^{-1}이상의 이론 용량을 가지며 간단한 과정을 통해 처리 및 재활용을 할 수 있습니다. 하지만, 이러한 유기 물질들은 액체 전해질에 녹아 급격한 용량 저하를 일으키며 물질 자체 전도도가 낮은 한계가 있어 이를 해결해야 하는 상황입니다.

그래서 본 연구에서는 Pillar[5]quinone (P5Q)이라는 유기물질을 양극 활물질로 사용한 연구를 진행하였습니다. 전극을 만들 때 다중벽 탄소 나노튜브 (MWCNT)와 셀룰로오스 나노파이버 (CNF)를 이용하여 활물질이 액체 전해질에 녹아 나가지 못하도록 하는 지지체로 사용하였고, 낮은 전도도 문제 또한 해결을 하였습니다. 전극은 진공 여과 방법을 통해 만들었는데, 이는 집전체가 필요하지 않아 가볍게 만들 수 있으며 활물질의 tap density를 높일 수 있습니다. 또한, 기존에 사용하고 있는 올레핀(olefin) 계열의 분리막을 대신하여 CNF를 분리막으로 사용하

는 시도를 하였습니다. 이를 통해, 높은 이온 전도도 (0.88 mS cm^{-1}), 전해질과의 높은 젖음성 (electrolyte uptake: 333.41 %, porosity: 70±5 %)과 열적 안전성까지 확보할 수 있었습니다. 따라서, P5Q 양극과 CNF 분리막을 적용한 리튬 금속 배터리는 올레핀 계열의 분리막을 적용한 배터리에 비해 안정적인 용량 유지 (76.5 % after 50 cycles at 0.2 C rate)와 더불어 향상된 율속 특성까지 보였습니다.

주요어: 유기 리튬 배터리, 셀룰로오스 나노파이버, 탄소 지지체, 친환경적인 리튬이온배터리, 차세대 배터리
학 번: 2017-20994